29th International Congress
on Sound and Vibration
The annual congress of
the International Institute
of Acoustics and Vibration (IIAV)

9–13 July 2023

ICSV29

A MODULAR LOW-MACH-NUMBER AXIAL-FLOW FAN TEST BENCH: IMPACT OF OUTLET-GUIDE-VANE HETEROGENEITY ON THE RADIATED NOISE

Antonio Pereira and Michel Roger
École Centrale de Lyon, France
e-mail: antonio.pereira@ec-lyon.fr

Fan noise is a significant contributor to the overall noise level of aircraft equipped with increased by-pass ratio engines. The impingement of the rotor wakes onto the downstream stator vanes is a major source among different noise generation mechanisms. Its contribution may be reduced by carefully choosing the number of rotor blades and stator vanes at initial design stage to ensure that generated spinning modes are cutoff by the duct at the first blade passing frequencies. However, due to structural constraints, the insertion of supporting struts or the modification of stator vanes may be required. Therefore, the periodicity of the rotor-stator interaction is modified and a regeneration of noise at the blade passing frequencies is expected. This paper presents an experimental study of the impact of stator heterogeneity on the rotor-stator interaction noise. Two different outlet-guide-vanes (OGV) sets are tested, a baseline one with 23 identical vanes and a heterogeneous OGV with 3 out of 23 vanes thickened due to structural reasons. The rotor consists of 17 identical blades that reach a tip Mach number of 0.3 at the nominal rotational speed. The rotor-stator stage is installed in the LP3 test bench at the Ecole Centrale de Lyon in France. It is a modular axial-flow ducted-fan test rig equipped with advanced instrumentation with up to 128 simultaneous acquisition channels. An acoustic characterization of the two OGV sets is performed via in-duct and far-field microphone arrays. The duct modal content is assessed both upstream and downstream of the rotor-stator stage. A far-field hemispherical array surrounding the duct intake is used to measure the directivity and estimate the sound power of the radiated noise. In addition it is used to validate a modal decomposition approach based on acoustic pressure measured in the far-field.
Keywords: mode detection, low-speed axial-flow fan, heterogeneous outlet-guide-vanes

1. Introduction

Choosing the number of rotor blades B and stator vanes V is a common practice to ensure a low-noise design of axial-flow ducted fans. A careful choice will result in rotor-stator wake-interaction modes [1] of high enough azimuthal orders that are cut-off by the duct at first blade passing frequencies (BPF). Nevertheless this reasoning is only valid for stages featuring blades and vanes of equal geometry. The increase of bypass ratio of recent turbofan engines resulted in shorter nacelles and the need of structural stator vanes or even struts downstream of the rotor. Thus, the periodicity of rotor-stator wake-impingement is modified and the regeneration of cut-on modes not predicted by the Tyler and Sofrin's rule will lead to unexpected tones [2]. This has been recently addressed by numerical simulations using a Lattice Boltzmann Method [3, 4]. In this work, an experimental study is carried out to assess the impact of heterogeneous

vanes on the noise radiated by a rotor-stator stage. Two sets of Outlet Guide Vanes (OGV) have been manufactured for this study. One with 23 identical vanes and a second one with 3 modified vanes out of 23. Both geometries are tested in a modular low-speed axial-flow fan test bench. Advanced instrumentation allows a precise control of the fan operating point and the modal content to be assessed both upstream and downstream of the stage. The experimental set-up is described in Section 2. The theoretical background of mode detection is recalled in Section 3 and the discussion of results is given in Section 4

2. Experimental set-up

2.1 Low Mach-number axial-flow test bench

An experimental test campaign has been carried out to assess the impact of heterogeneous outlet guide vanes (OGV) on the radiated noise. Two stator rows consisting of 23 vanes have been manufactured by Safran Ventilation Systems. One with 23 vanes of equal geometry, hereafter called homogeneous OGV, and a second with 3 modified vanes out of 23, called heterogeneous OGV. The 3 modified vanes consist of the baseline one with a linear increase of thickness from the hub to the vane tip. Thus, at the hub both geometries are equal and at the tip the modified vanes are thickened by a factor of 3. The rotor consists of 17 identical blades that reach a tip Mach number of about 0.3 at the nominal speed.

The rotor-stator stage is installed in a test-rig run by the Ecole Centrale de Lyon in France, see the sketch in Fig. 1. It is a modular low-Mach-number axial-flow test bench. The duct diameter is 17cm and the maximum mass-flow rate is 1 kg/s at the nominal rotation speed which is about 10000 rpm.

The test-bench is equipped with a Turbulent Control Screen (TCS) to avoid inlet vortical flow structures to interact with rotor blades [5]. The mass-flow rate is measured by a Venturi tube system downstream of the rotor-stator stage. The air then passes through an anechoic settling chamber that minimizes the test-section contamination from duct-end reflections. A gate-valve is placed downstream of the acoustic plenum and allows to control the operating point of the stage. A series of static pressure sensors are used to measure the pressure rise due to the fan as well as the pressure drop due to the constriction in the Venturi tube.

The rotor-stator stage is mounted in a axial portion of the duct that can be easily disassembled from the main duct. The stator row is a single block piece that supports both the rotor and the electric motor on the duct casing. For the comparison of the two OGV configurations the performance of the stage is controlled in real-time and the same operating point is tackled for both configurations such as to ensure the same aerodynamic load. The performance chart is given in Fig. 2 for the two OGV configurations at different rotational speeds.

2.2 Instrumentation for mode detection

The test rig is equipped with different microphone arrays. In the present configuration, two identical in-duct arrays consisting of 25 non-uniformly located microphones are installed both upstream and downstream of the rotor-stator stage. These arrays have been optimized to provide a complete modal-breakdown up to the third Blade Passing Frequency (BPF) at the nominal rotational speed, thus a Helmholtz number of about $kR_2 = 15$. Brüel & Kjaer type 4957 microphones are wall-flush mounted using a pin-hole system. All microphones are calibrated both in amplitude and phase using the approach detailed in ref. [6]. For that, 13 circularly placed loudspeakers are used to excite an artificial modal content at position of the array microphones, see Fig. 1. Pressure time signals are acquired simultaneously using a 128-channel B&K data acquisition system. Finally, a laser tachometer probe is used to measure the instantaneous rotational speed.

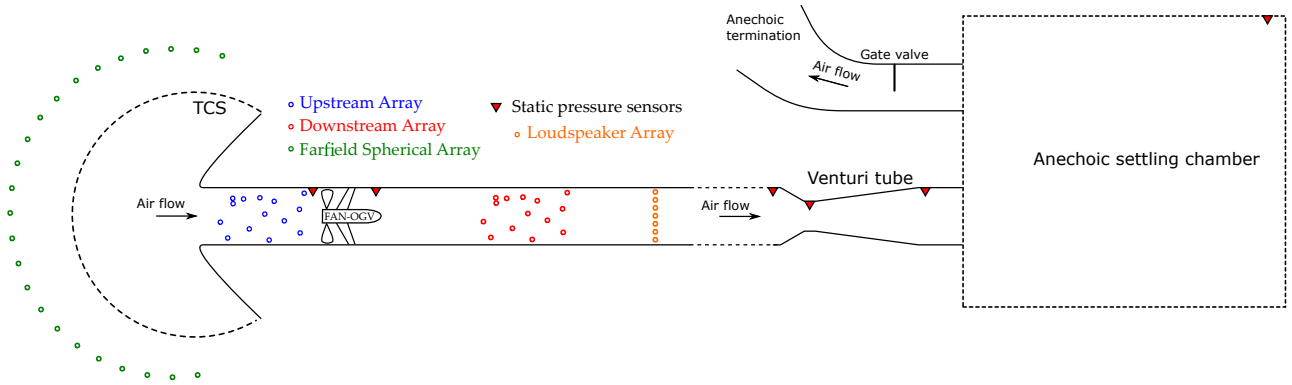

Figure 1: Sketch of the test-rig on which the LP3 rotor-stator stage is installed. The air is sucked by the fan and passes through the Turbulent Control Screen (TCS). Static pressure sensors measure the pressure rise due to the rotor/stator stage as well as static pressures for computing the mass flow rate by the Venturi tube. A loudspeaker array is used for the calibrating pin-hole mounted microphones. Upstream and downstream duct modal content is assessed by in-duct microphone arrays.

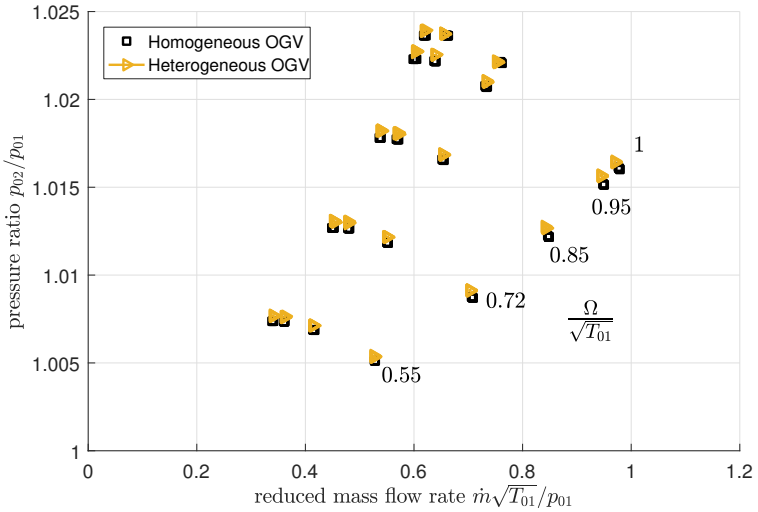

Figure 2: Performance chart of the LP3 axial-flow fan for both the homogeneous and the heterogeneous OGV configurations at different rotational speeds. p_{01} and T_{01} are both the ambient static pressure and temperature, whereas p_{02} is the static pressure downstream of the stage and $\dot{m}$ is the mass-flow rate.

3. Outline of theory - mode detection

In this section the in-duct formulation of the acoustic pressure field is briefly recalled. Both upstream and downstream in-duct microphone arrays are located in a hard-walled duct with constant circular cross-section. This allows the acoustic pressure $\hat{p}$ to be expanded into a sum of duct modes in a cylindrical coordinate system as follows

$$\hat{p}(z,r,\phi) = \sum_{m=-\infty}^{\infty} \sum_{j=0}^{\infty} \left[A_{mj}^{+} \mathrm{e}^{\mathrm{i}\gamma_{nj}^{+} z} + A_{mj}^{-} \mathrm{e}^{\mathrm{i}\gamma_{nj}^{-} z} \right] f_{nj}(r) \mathrm{e}^{\mathrm{i}m\phi}, \tag{1}$$

with $n = |m|$, A_{mj}^{+} and A_{mj}^{-} being complex-valued amplitudes of downstream and upstream modes of azimuthal order m and radial order j. The radial shape factor $f_{nj}(r)$ for a circular cross-section is

$$f_{nj}(r) = \frac{J_{|m|}(K_{nj}r)}{\Gamma_{nj}}, \tag{2}$$

with $J_{|m|}$ the m-th order Bessel function of first type, K_{nj} a radial wave-number determined by the boundary conditions and Γ_{nj} a normalization factor given by

$$\Gamma_{nj} = \sqrt{\left(1 - \frac{m^2}{(K_{nj}R_2)^2}\right) J_{|m|}^2(K_{nj}R_2)}, \tag{3}$$

with R_2 the inner radius of the duct casing. The axial wavenumbers $\gamma_{nj}^{\pm}$ in both downstream and upstream directions are written

$$\gamma_{nj}^{\pm} = \frac{1}{\beta_a^2}\left(-M_a k \pm \sqrt{k^2 - \beta_a^2 K_{nj}^2}\right), \tag{4}$$

where $M_a = W_0/c_0$ is the axial Mach number of a mean flow with uniform axial velocity W_0 and c_0 is the sound speed. The acoustic wavenumber is $k = \omega/c_0$ with ω the angular frequency and $\beta_a = \sqrt{1 - M_a^2}$ is the Prandtl-Glauert factor. Assuming that array microphones are located relatively far away of the sources and duct discontinuities, the summation in Eq. (1) might be truncated to consider only cut-on modes. The principle of mode detection approaches is to spatially sample the in-duct sound pressure and estimate the modal coefficients A_{mj}^{+} and A_{mj}^{-} for a given model of the sound field as given by Eq. (1) for the case of hard-walled duct of circular cross-section. Equation (1) can be conveniently written in matrix form as

$$\mathbf{p} = \mathbf{\Phi}\mathbf{a}, \tag{5}$$

with $\mathbf{p} \in \mathbb{C}^K$ a vector of complex pressure (as returned from a Fourier transform) at frequency ω at K microphone positions, $\mathbf{a} \in \mathbb{C}^L$ a vector containing the *unknown* complex mode coefficients and $\mathbf{\Phi} \in \mathbb{C}^{K\times L}$ a matrix whose entries are determined from Eq. (1). As discussed in the previous section, the test-rig is equipped with optimized non-uniform microphone arrays that allow a complete modal breakdown into both azimuthal and radial modes. In addition, it allows to single-out upstream and downstream propagating modes. Considering that N_m and N_j are respectively the highest azimuthal and radial orders that propagate without attenuation, the dimension L is equal to $2(N_j + 1)(2N_m + 1)$. Acquisition of the sound pressure is carried out at stationary conditions for a fixed operating point as shown in Fig. 2. The measured time signals might be assumed stationary and ergodic, allowing one to express Eq. (5) in terms of the cross-spectral matrix of measurements $\mathbf{S_{pp}} \triangleq \mathbb{E}\{\mathbf{p}\mathbf{p}^H\}$, where $\cdot^H$ is the conjugate transpose or the Hermitian of a vector and $\mathbb{E}\{\cdot\}$ the expected value. Equation (5) writes

$$\mathbf{S_{pp}} = \mathbf{\Phi}\mathbf{S_{aa}}\mathbf{\Phi}^H. \tag{6}$$

The goal of mode detection approaches is to determine $\mathbf{S_{aa}}$ from the knowledge of $\mathbf{\Phi}$ and the measurements $\mathbf{S_{pp}}$. An estimate of $\mathbf{S_{aa}}$ is obtained here by an iterative Bayesian Inverse Approach (iBIA) [7], recently applied for analyzing the modal content of fan broadband noise [8]. Once the modal coefficients are estimated, the sound power carried by each mode can be estimated by

$$W_{mj}^{\pm} = \frac{kS\beta_a^4}{2Z_0} \frac{\sqrt{k^2 - \beta_a^2 K_{nj}^2}}{\left(k \mp M_a\sqrt{k^2 - \beta_a^2 K_{nj}^2}\right)^2} \left|A_{mj}^{\pm}\right|^2, \tag{7}$$

where $S = \pi R_2^2$ is the duct cross-section surface where the mode detection is carried and $Z_0 = \rho_0 c_0$ is the acoustic impedance. The total duct sound power transmitted both upstream and downstream of the rotor-stator stage is determined by summing over the azimuthal and radial orders

$$W^{\pm} = \frac{kS\beta_a^4}{2Z_0} \sum_{m=-N_m}^{N_m} \sum_{j=0}^{N_j} \frac{\sqrt{k^2 - \beta_a^2 K_{nj}^2}}{\left(k \mp M_a \sqrt{k^2 - \beta_a^2 K_{nj}^2}\right)^2} \left|A_{mj}^{\pm}\right|^2 . \tag{8}$$

4. Results and discussion

An acoustic characterization has been performed for the set of operating points shown in Fig. 2. In this work, focus will be given to the highest mass-flow rate point at nominal rotation speed which is about 10,000 rpm. First, wall-pressure fluctuations spectra averaged over both upstream and downstream microphone arrays are shown in Fig. 3. The results compare the heterogeneous against the homogeneous OGV configuration. At the first BPF, the stator with heterogeneity leads to an increase of 9 dB upstream and 12 dB downstream. For the second BPF the increase is about 3 dB upstream and 8 dB downstream. Levels at the third harmonic of the BPF show a slight increase both upstream (less than 1 dB) and downstream (about 2 dB). This is expected since the rotor-stator wake-interaction noise for the $B = 17$ and $V = 23$ configuration is cut-on at BPF3 for the studied homogeneous configuration. Thus, the effect of heterogeneity is expected to be minor. It can be seen in Fig. 3 that broadband levels are almost unchanged between homogeneous and heterogeneous configurations. This is also expected due to the fact that broadband sources are uncorrelated and less sensitive to geometrical irregularities. Residual noise levels are still observed at the BPF and first harmonic. This indicates that another mechanism such as flow separation regenerates cut-on modes. Further investigation is needed to confirm that hypothesis.

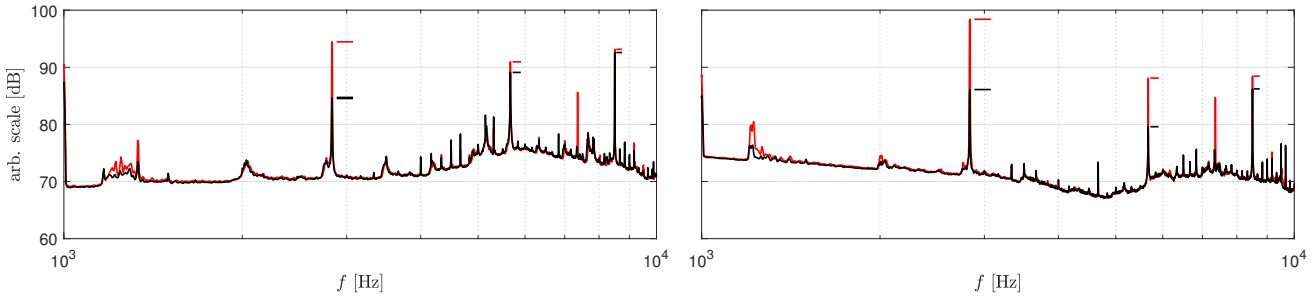

(a) upstream (b) downstream

Figure 3: Spectra of wall-pressure fluctuations measured (a) upstream and (b) downstream of the LP3 fan for the homogeneous OGV (black) and the heterogeneous OGV (red). The spectra consists of the average over the set of microphones in both the upstream and downstream arrays, see Fig. 1.

A modal-breakdown has been carried out by the approach presented in the previous section. Modal coefficients $A_{mj}^{\pm}$ are estimated both upstream and downstream of the fan. The acoustic power carried by each mode is then estimated using Eq. (7). The sound power transmitted against the flow direction W_{mj}^{-} is shown for the upstream array whereas for the downstream array the results are given for W_{mj}^{+}, that is, modes propagating in the flow direction. The modal content upstream of the rotor is shown in Fig. 4. At the first BPF, the heterogeneous OGV configuration leads to the emergence of two dominant modes $m = -3$ and 3 as compared to the homogeneous case. The total sound power level is seen to increase by more than 6 dB. Results at twice the BPF, see Fig. 4(b), show the emergence of modes $m = -3, 3$

and 5 for the heterogeneous OGV case. Finally, at the third BPF the rotor-stator wake-interaction mode predicted by Tyler and Sofrin's rule $m = 5$ carries the majority of energy and additional modes are observed for the heterogeneous OGV, see $m = 8$ and 11. A great part of these modes might be predicted by means of an analytical modeling of the heterogeneity, this is shown in an accompanying paper [9].

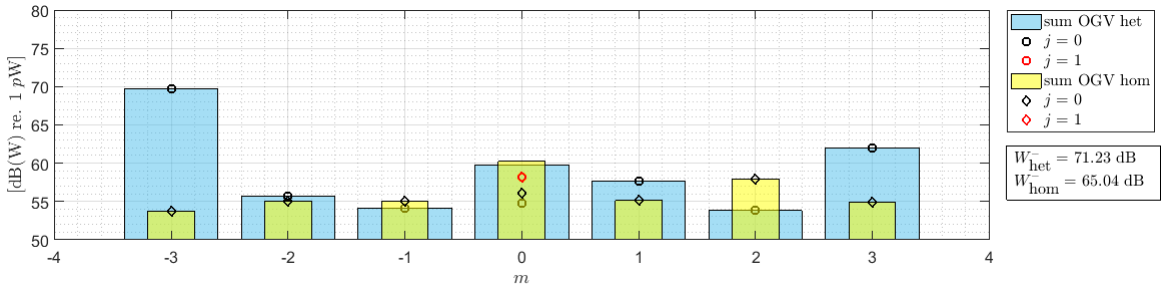

(a) BPF1

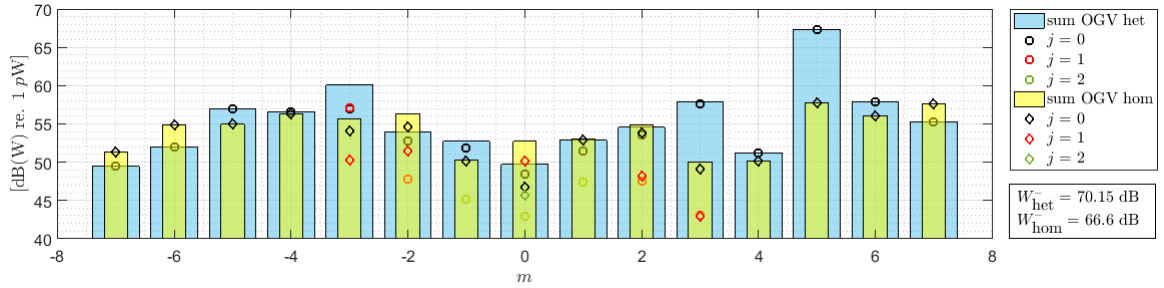

(b) BPF2

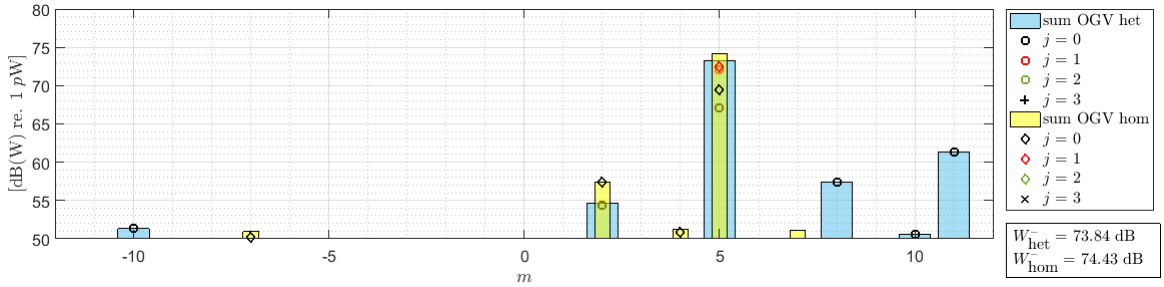

(c) BPF3

Figure 4: Modal breakdown of the sound field measured upstream of the rotor-stator stage for both homogeneous (yellow) and heterogeneous (blue) OGV configurations. The bar levels give the contribution summed over radial orders j, that is, $W^-_m = \sum_{j=0}^{N_j} W^-_{mj}$. The modal sound powers for individual radial orders W^-_{mj} are given by colored symbols according to the legend on the right-hand side. The total in-duct sound power transmitted upstream is given by W^-_{het} and W^-_{hom} for the heterogeneous and homogeneous OGV respectively.

The modal content downstream of the rotor-stator stage is shown in Fig. 5. Several modes are regenerated at the BPF for the heterogeneous OGV, the $m = -3$ being the dominant one as for the upstream case. The total sound power is increased by more than 9 dB as compared to the homogeneous case. At twice the BPF, modes $m = 5, -6, -5, -4, -3$ and -2 are regenerated. Contrary to the upstream modal content, the majority of additional modes are counter-rotating. This might be due to the fact that the main radiation lobe of equivalent dipoles placed at the stator leading edge are well aligned with counter-rotating modes downstream. Thus, these modes are expected to radiate more efficiently downstream of the fan. Finally, for the third BPF, the $m = 5$ is the dominant mode with other spurious modes for the

heterogeneous OGV, such as the $m = -10, -9, -6$ and -4.

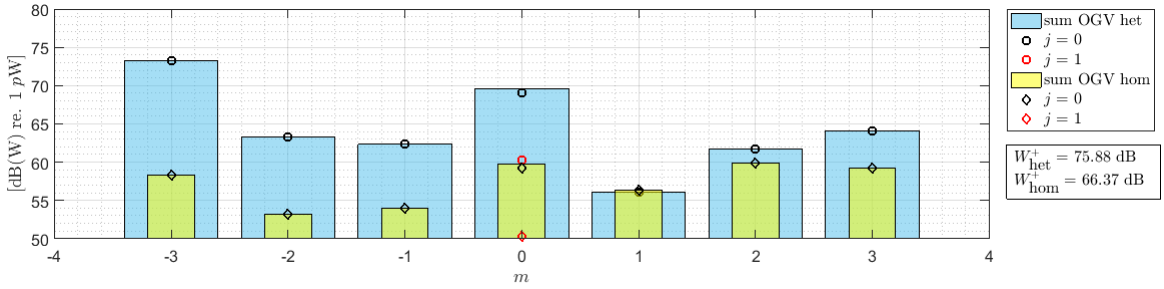

(a) BPF1

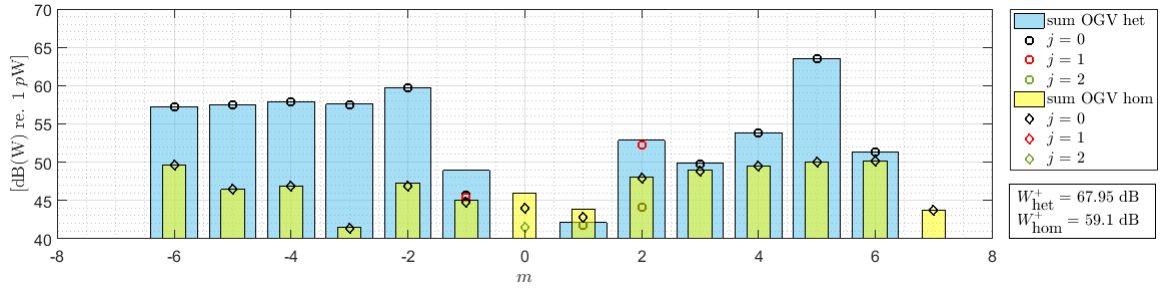

(b) BPF2

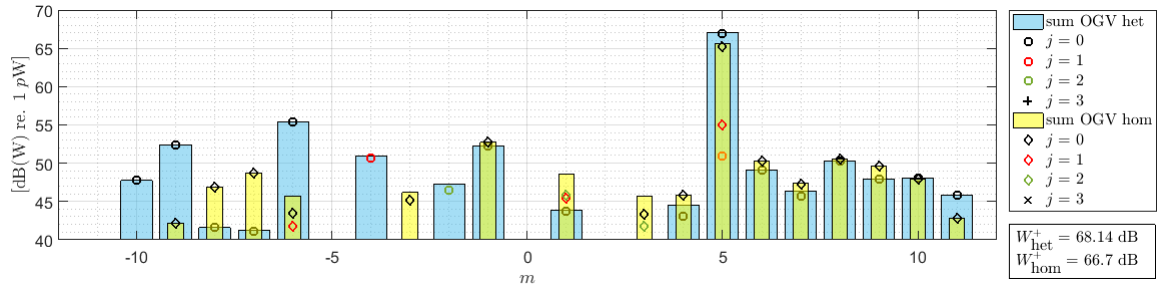

(c) BPF3

Figure 5: Modal breakdown of the sound field measured downstream of the rotor-stator stage for both homogeneous (yellow) and heterogeneous (blue) OGV configurations. The bar levels give the contribution summed over radial orders j, that is, $W^+_m = \sum_{j=0}^{N_j} W^+_{mj}$. The modal sound powers for individual radial orders W^+_{mj} are given by colored symbols according to the legend on the right-hand side. The total in-duct sound power transmitted downstream is given by W^+_{het} and W^+_{hom} for the heterogeneous and homogeneous OGV respectively.

5. Conclusion and perspectives

The impact of heterogeneous stator vanes has been studied experimentally through a low-speed axial-flow test bench. Two OGV sets have been tested: one with identical vanes and a second with heterogeneous vanes. Acoustic characterization of both geometries has shown that even small heterogeneity can lead to strong increase of tonal noise levels. At the BPF, augmentations reaching 9 dB upstream and 12 dB downstream have been measured.

The in-duct modal content has been assessed both upstream and downstream of the rotor-stator stage up to the third BPF. It was shown that new dominant modes are regenerated for the heterogeneous configuration. Downstream of the heterogeneous OGV, higher power levels are observed for counter-rotating

modes at BPF2 and BPF3 as compared to upstream. The study has shown a minor effect of heterogeneity on broadband levels as well as for modes that are already cut-on in a homogeneous design.

Unexpected residual noise levels are observed at the BPF and first harmonic for the homogeneous OGV. This suggests that other mechanisms such as flow separations might contribute to the generated noise. For a better understanding, the measurement of flow conditions behind the rotor would be of value.

Acknowledgements

The presented work was conducted within the framework of the industrial chair ARENA (ANR-18-CHIN-0004-01) co-financed by Safran Aircraft Engines and the French National Research Agency (ANR) and in the framework of the Labex CeLyA (ANR-10-LABX-0060) of the Université de Lyon, within the program "Investissements d'Avenir" (ANR-16-IDEX-0005) operated by the French National Research Agency (ANR). Emmanuel Jondeau, Jean-Charles Vingiano, Pascal Souchotte and Edouard Salze are kindly acknowledge for their help in setting up the experiment.

REFERENCES

1. Tyler, M. and Sofrin, T. G. Axial flow compressor noise studies, *Society of Automotive Engineers Transactions*, **70**, 309–332, (1962).

2. Roger, M. and Caule, P. Assessment of the effect of stator inhomogeneity on rotor-stator tonal noise, *15th International Symposium on Transport Phenomena and Dynamics of Rotating Machinery, ISROMAC-15, Honolulu, HI*, (2014).

3. Sanjosé, M., Moreau, S., Pestana, M. and Roger, M. Effect of weak outlet-guide-vane heterogeneity on rotor–stator tonal noise, *AIAA Journal*, **55** (10), 3440–3457, (2017).

4. Pestana, M., *Effets d'un stator hétérogène sur le bruit d'interaction rotor-stator: étude analytique, expérimentale et numérique*, 2020LYSEC003, École Centrale de Lyon, (2020).

5. Pestana, M., et al. Aeroacoustics of an axial ducted low mach-number stage: numerical and experimental investigation, *Proceedings of the 23rd AIAA/CEAS Aeroacoustics Conference*, no. No. 2017-3215, (2017).

6. Leclère, Q., Pereira, A., Finez, A. and Souchotte, P. Indirect calibration of a large microphone array for in-duct acoustic measurements, *Journal of Sound and Vibration*, **376**, 48 – 59, (2016).

7. Leclère, Q., Pereira, A., Bailly, C., Antoni, J. and Picard, C. A unified formalism for acoustic imaging based on microphone array measurements, *International Journal of Aeroacoustics*, **16** (4-5), 431–456, (2017).

8. Pereira, A. and Jacob, M. C. Modal analysis of in-duct fan broadband noise via an iterative bayesian inverse approach, *Journal of Sound and Vibration*, **520**, 116633, (2022).

9. Roger, M. and Pereira, A. Regeneration of ducted rotor-stator wake-interaction tonal noise because of vane-to-vane irregularities, *ICSV-29, Prague*, (2023).